Zhiyu Yan, Hong Zhao*, Baozhong Han*, Jiaming Yang and Junqi Chen

The suppression of space charge accumulation in CB/LDPE nanocomposites and its association with molecule relaxation

https://doi.org/10.1515/epoly-2017-0111
Received June 7, 2017; accepted September 5, 2017; previously published online October 31, 2017

Abstract: Space charge accumulation within insulating material poses a threat to the reliability in the operation of DC power cables. To investigate the influence of carbon black (CB) on the space charge accumulation of low density polyethylene (LDPE), both conductive carbon black (C-CB) and insulating carbon black (I-CB) were employed as filler particles. The space charge distributions of LDPE and CB/LDPE nanocomposites were obtained by the pulsed electro-acoustic (PEA) method. Additionally, dynamic mechanical analysis (DMA) and thermally stimulated current (TSC) spectroscopy were applied to explore the mechanism of improving space charge performance. Both the C-CB/LDPE and I-CB/LDPE nanocomposites can effectively suppress space charge accumulation. It was concluded that the improvement in space charge characteristics of CB/LDPE nanocomposites was attributable to the interaction between the CB particles and the LDPE, which reduces the number of defects formed from molecules participating in α relaxation and decreases the density of traps within the LDPE.

Keywords: CB/LDPE nanocomposites; dynamic mechanical analysis; α relaxation; space charge; thermally stimulated current.

***Corresponding authors: Hong Zhao,** Key Laboratory of Engineering Dielectric and its Application, Ministry of Education, Harbin University of Science and Technology, Harbin 150080, China, e-mail: hongzhao@hrbust.edu.cn; and
Baozhong Han, Key Laboratory of Engineering Dielectric and its Application, Ministry of Education, Harbin University of Science and Technology, Harbin 150080, China; and Shanghai Qifan Wire and Cable Co., Ltd., Shanghai 200008, China, e-mail: hbzhlj@163.com
Zhiyu Yan: Key Laboratory of Engineering Dielectric and its Application, Ministry of Education, Harbin University of Science and Technology, Harbin 150080, China; and Zhongtian Technology Submarine Cables Co., Ltd., Nantong 226010, China
Jiaming Yang and Junqi Chen: Key Laboratory of Engineering Dielectric and its Application, Ministry of Education, Harbin University of Science and Technology, Harbin 150080, China

1 Introduction

Flexible direct current (DC) power transmission is widely used due to offshore developments and renewable energy utilization. Therefore, the DC high voltage cables are applied extensively as key apparatus in flexible DC transmission systems (1, 2). Polyethylene has been widely employed as power cable insulation material for its excellent dielectric and electrical insulation properties (3, 4). However, polyethylene exhibits the phenomenon of space charge accumulation in DC high voltage transmission applications, which severely limits its use and development in DC high voltage cables. Space charge accumulation can cause a local electrical field strength increase in the insulation layer, leading to reduction in the service life of such cables and even may cause breakdown of the insulation (5–7). Many researchers dedicated efforts to suppressing space charge accumulation through modifying polyethylene and it has been demonstrated that the addition of inorganic nanoparticles can enhance the space charge performance (8–12). Nanoparticles have some special physical properties that differ from ordinary materials because of their larger surface energy and high specific surface area (13). Consequently, the addition of nanoparticles has become an effective way to improve the space charge characteristics of such polymers.

As nanotechnology has been developed the mechanism to improve dielectric properties of the polymer with nanoparticles was ceaselessly explored. The multi-core model was proposed by Tanaka, who considered that there is an interface region between nanoparticles and the polymer matrix (14). The interface region is composed of a bonded layer, a bound layer and a loose layer. The multi-core model proposed to some extent the mechanism of significant improvement in dielectric properties of the nanocomposite, but to date the interface structure had not been confirmed by experiments. Lewis and Nelson predicted that an interface charge layer might exist between the nanoparticles and the polymer matrix, based on the theory of suspension chemistry (15, 16). It has been hypothesized that the regulatory effect of interface charge layer plays an important role in modifying the

electrical properties of the nanocomposite. Yang found that the interface charge layer existed in an SiO_2/LDPE nanocomposite. However, there was no obvious interface charge layer in MgO/LDPE nanocomposites. Nevertheless, both nanocomposites can effectively suppress space charge accumulation (17). It has been suggested that the interface charge layer is not the dominant factor affecting the space charge property. Although many experimental results have been obtained and some models have been proposed, the mechanism of suppressing space charge accumulation of nanocomposites is still not very clear. The relationship between space charge behaviors and microstructure is still lacking sufficient understanding, and research about the impact of molecular relaxation on the space charge accumulation is rarely reported.

During the present investigation, the mechanism of suppressing space charge accumulation was explored from the viewpoint of the relationship between molecular relaxation and space charge behavior. Carbon black (CB) is a kind of natural nanoparticle with high specific surface area and surface activation energy that is widely used in the rubber industry as a reinforcing agent (18). Additionally, CB is also employed in conductive polymer composites. According to percolation theory, the CB particles can form a conductive network in the polymer matrix as the content of CB exceeds the percolation threshold, and it then makes the insulation polymer change into a conductor (19). However, the investigation of dielectric properties is rarely reported about polymers with small proportions of added CB particles. It would be of great interest to investigate such materials, which could gain better dielectric performance. The conductive CB (C-CB) and insulating CB (I-CB) were selected as filler particles, and a study was initiated into the effect of the CB on the space charge characteristics of low density polyethylene (LDPE). Additionally, the dynamic mechanical analysis (DMA) and thermally stimulated current (TSC) methods were introduced to explore the mechanism by which to improve the space charge performance of LDPE.

2 Experiment

2.1 Characterization of CB particles

The C-CB particles were obtained from the Degussa Company (Germany), model XE2-B, and the I-CB particles were obtained from Cabot Corporation (USA), model M-L. A JEM-2100 transmission electron microscope (TEM) (JEOL Corporation, Japan), was employed to observe the microstructure of the two kinds of CB particles. Firstly, the CB particles were dispersed in alcohol under ultrasonic vibration for 10 min to prepare a suspension. Then a small amount of the suspension was selected and observed. The Fourier transform infrared (FTIR) spectra were obtained using a Jasco FTIR-6100 FTIR spectrometer (JASCO Corporation, Japan) in the range from 4000 to 500 cm^{-1}. Both types of CB particles were uniformly mixed with KBr powder and then compressed into films. The samples were tested using the transmission mode. The background count of the atmosphere was measured and subtracted from each spectrum. X-ray photoelectron spectroscopy (XPS), type ESCALAB 250Xi (Thermo Scientific Escalab, USA) was used to analyze the content of carbon and oxygen for the C-CB and I-CB particles. A Hitachi SU8020 high resolution scanning electron microscope (SEM) (Hitachi, Japan), which can operate at a low accelerating voltage to limit charge accumulation and has strong ability of imaging, was selected to observe the dispersion of CB particles in the LDPE matrix.

2.2 Preparation of samples

LDPE (LD200) was obtained from SINOPEC Engineering (Group) Co., Ltd. (China). The CB particles and LDPE were melt-blended using a synclastic parallel twin-screw mixing extruder at 115°C to prepare the C-CB/LDPE and I-CB/LDPE nanocomposites with 1 phr (per 100 g resin add 1 g CB) CB. The samples were hot pressed molded at 115°C and 10 MPa using a flat vulcanizing machine. The samples were cooled to the room temperature under the same pressure. All of the samples were annealed in the vacuum oven at 80°C for 24 h to eliminate the thermal history and internal stress.

2.3 Measurement of space charge

The space charge distribution of each sample was measured using the pulsed electro-acoustic (PEA) method. The sensitivity and the spatial resolution of the PEA test system was 0.6 $\mu C/m^3$ and 18 μm, respectively. The average thickness of the samples was 300 μm and aluminum electrodes 25 mm in diameter were evaporated on both sides of the samples. A DC electrical field of 40 kV/mm was applied to the samples during the process of testing. The measurements were carried out for 30 min at room temperature and the space charge distribution of each sample was recorded every 1 min to track the development of any space charge accumulation.

2.4 Measurement of DMA

The dynamic mechanical properties of the LDPE and two kinds of nanocomposites were tested using a DMTA-IV DMA cantilever beam model at a 1 Hz vibration frequency and 15 μm amplitude. The measurements were performed over the temperature range from room temperature to 90°C with a temperature increase of 3°C/min.

2.5 Measurement of TSC

The TSC measurement was performed for LDPE and its nanocomposites. Film samples 100 μm in thickness were poled with a 4000 V DC voltage at room temperature for 30 min and were then cooled rapidly with the application of a poling voltage. When the samples had been cooled below 0°C the poling voltage was removed and the external circuit was shorted. As the short current decayed to 1 pA, the temperature was increased from 0°C to 90°C at rate of increase of 3°C/min. The external current was measured as a function of temperature.

3 Results

3.1 Characteristic results of CB particles

The TEM images of both C-CB and I-CB particles are shown in Figure 1. The difference between aggregate structures of the both particles is readily evident. The C-CB primary particles attach to each other to form an aggregate with a larger number of longer branched structures. However, the aggregate of I-CB was similar to "grape clusters".

The FTIR spectra of C-CB and I-CB are shown in Figure 2. As is evident from Figure 2, both types of CB particles exhibit almost the same absorption peaks at 3440, 2925, 2856, 2359, 1640, 1392 and 1082 cm^{-1}. This indicates that the two types of CB have some similar surface groups. By reference to the position of the absorption peaks the type of surface group can be determined. The absorption peak at 3440 cm^{-1} represents the typical stretching vibration of -OH. The absorption peaks located at around 2925 cm^{-1} and 2856 cm^{-1} represent the C-H bond. The peak at 2359 cm^{-1} is caused by CO_2 that is absorbed by CB and KBr. Absorption peaks at 1640 cm^{-1}, 1392 cm^{-1} and 1082 cm^{-1} correspond to C=O, -COO- and aromatic ethers, respectively (20). It is clearly evident that strength of the absorption peaks of I-CB at 3440, 1640 and 1392 cm^{-1} are stronger than that of C-CB and in consequence it can be concluded that the I-CB particle has more surface groups (21).

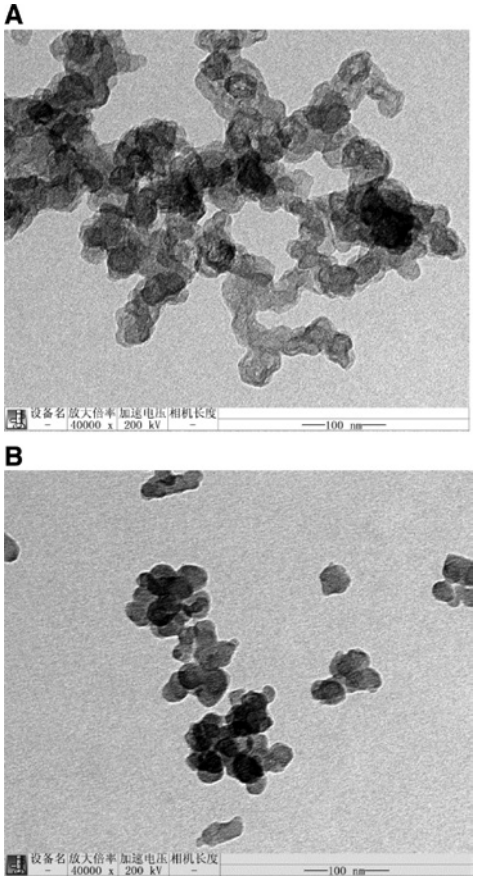

Figure 1: TEM images of C-CB and I-CB particles. (A) C-CB and (B) I-CB.

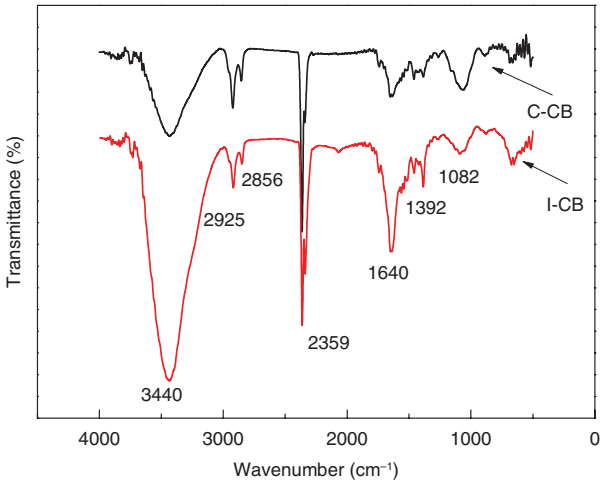

Figure 2: FTIR spectra of C-CB and I-CB.

XPS spectra of the two types of CB particles are shown in Figure 3. There are two peaks at 284.6 eV and 532.6 eV that correspond to the C1s peak and O1s peak, respectively.

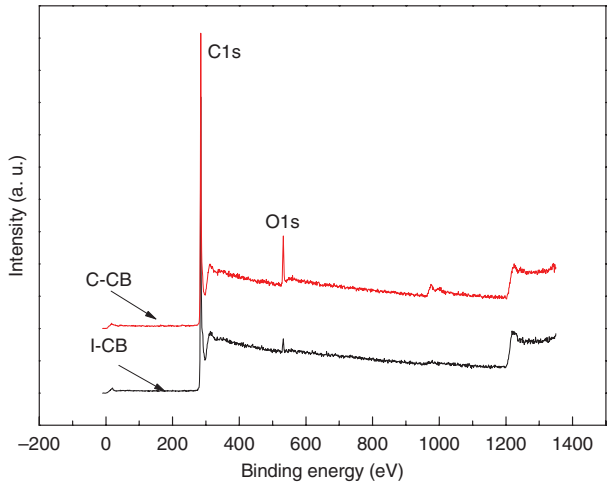

Figure 3: XPS spectra of C-CB and I-CB.

The relative content of carbon and oxygen of the C-CB particles is 97.8% and 2.2%, respectively. For the I-CB particles, the relative content of carbon and oxygen is 92.6% and 7.4%, respectively. The oxygen content of I-CB is significantly higher than that of C-CB, which indicates that more oxygen groups are located on the surface of I-CB, and this result is consistent with the FTIR test results.

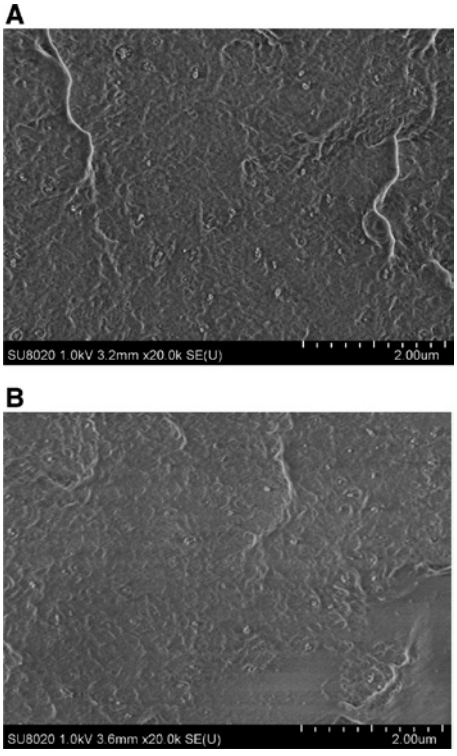

Figure 4: SEM pictures of C-CB/LDPE and I-CB/LDPE nanocomposites. (A) C-CB/LDPE and (B) I-CB/LDPE.

The nanocomposites were first hot-pressed into squares with a thickness of 1 mm and were then embrittled in liquid nitrogen and snapped off manually. Observations then were carried out on the fractured surface of the nanocomposite. The dispersion of CB particles in the C-CB/LDPE and I-CB/LDPE nanocomposites, as viewed at an accelerating voltage of 1 kV, are shown in Figure 4. It can be observed that both types of nanoparticles are dispersed uniformly in the LDPE matrix, and that the particle size is <100 nm.

3.2 Space charge measurement results

The space charge distribution of LDPE under an electrical field of 40 kV/mm is shown in Figure 5A. After the stress is applied for 30 min, there is significant space charge accumulation in the LDPE sample and the amount of space charge gradually increases with increase in exposure time. In the case of the C-CB/LDPE nanocomposite, see Figure 5B, only a small amount of space charge can be observed in the middle of the sample and the accumulative charge remains almost unchanged for the duration of the test period. The amount of space charge is appreciably less than that of pure LDPE. The space charge distribution of I-CB/LDPE nanocomposite is shown in Figure 5C. There is a small space charge accumulation near the cathode within the sample. Although the amount of space charge within the I-CB/LDPE nanocomposite is more than that of the C-CB/LDPE nanocomposite, it is also significantly less than that of pure LDPE. From the space charge test results it is clear that space charge can be suppressed by addition of CB nanoparticles, and the C-CB/LDPE nanocomposite has the stronger ability to suppress space charge accumulation, as compared with the I-CB/LDPE nanocomposite.

3.3 DMA measurement results

The space charge property of a polymer is closely related to its microstructure. In order to establish the relationship between space charge behavior and microstructure, a dynamic mechanical experiment was performed to determine the storage modulus E′ and the loss factor tan δ as a function of temperature for LDPE, C-CB/LDPE and I-CB/LDPE nanocomposites. The storage modulus E′ is one of the important indicators for material rigidity, and the loss factor tan δ can characterize the relaxation of the material. The storage modulus E′ of the three kinds of materials are shown in Figure 6A. As shown in Figure 6A, the

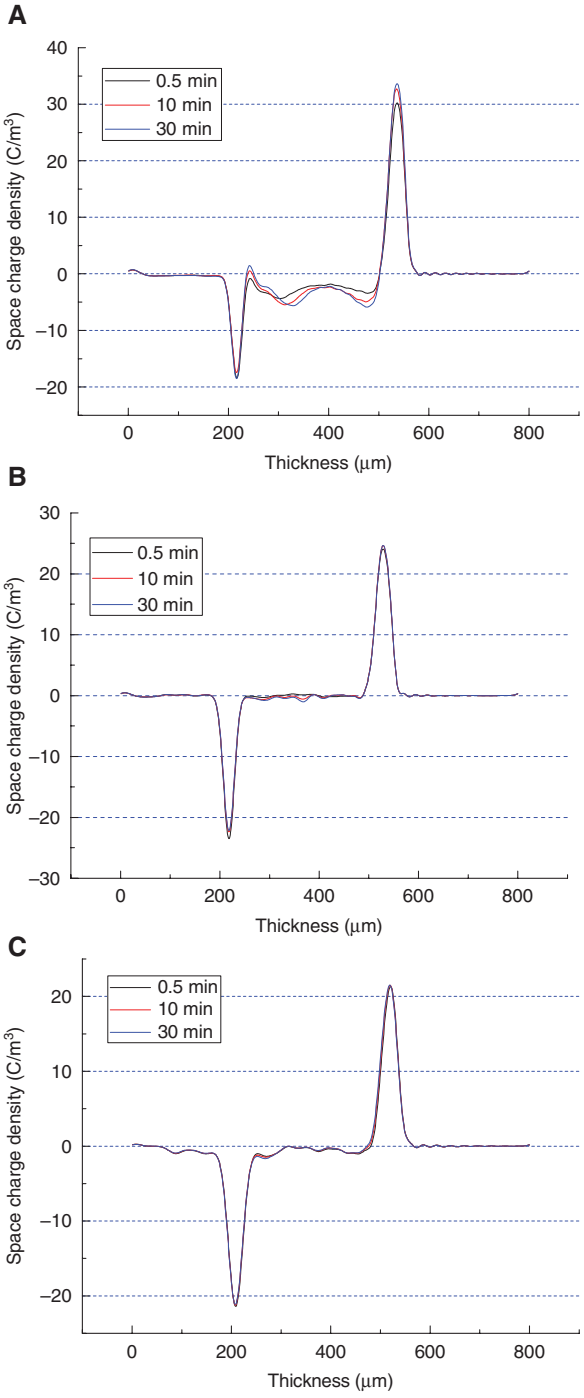

Figure 5: Space charge distribution of LDPE and CB/LDPE nanocomposites.
(A) LDPE, (B) C-CB/LDPE and (C) I-CB/LDPE.

storage modulus E′ could be increased by the addition of CB particles over the temperature range of the test, and the results for the C-CB/LDPE nanocomposite was higher than for that of the I-CB/LDPE nanocomposite. Figure 6B shows the loss factor tan δ for LDPE and its nanocomposites. It can be observed that the loss factor tan δ differed

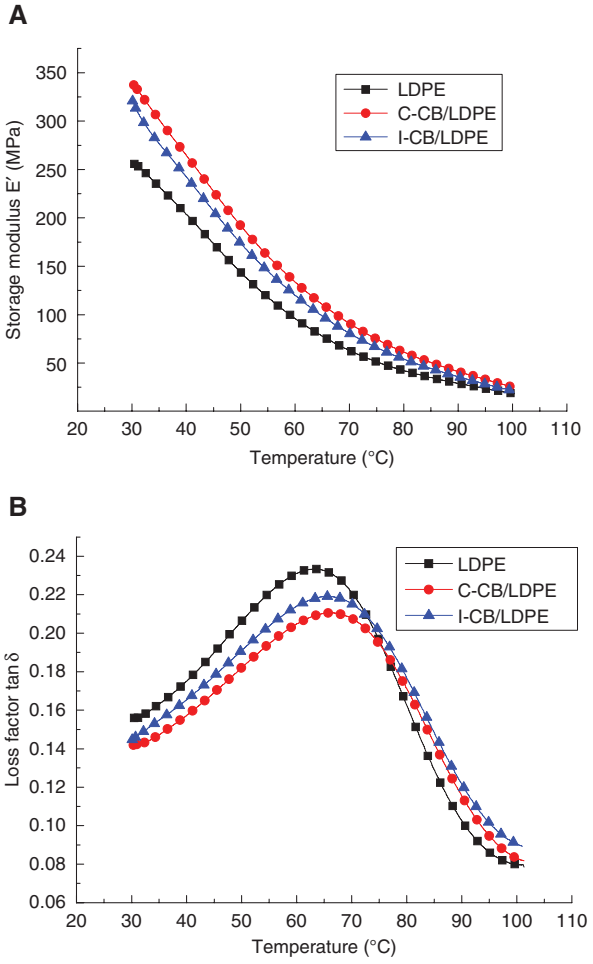

Figure 6: Temperature dependence of E′ and tan δ for LDPE and the CB/LDPE nanocomposites.
(A) Storage modulus, (B) loss factor.

for each of the three kinds of materials. The peak value of the loss factor tan δ gradually decreased in the order of LDPE, I-CB/LDPE nanocomposite and C-CB/LDPE nanocomposite. In addition, the peak position of loss factor tan δ shifted to the higher temperature region for both of the nanocomposites.

3.4 TSC measurement results

The results of the TSC tests are shown in Figure 7. It was determined that the TSC current peak of LDPE occurred at approximately 65°C, and that the peak value reached 24 pA. For C-CB/LDPE and I-CB/LDPE nanocomposites, the value of the TSC current peak around 65°C was less than that for LDPE, and the corresponding peak values were 7 pA and 12 pA, respectively. It was also observed that for the two kinds of nanocomposites there was a new TSC current peak in high temperature region at about 85°C.

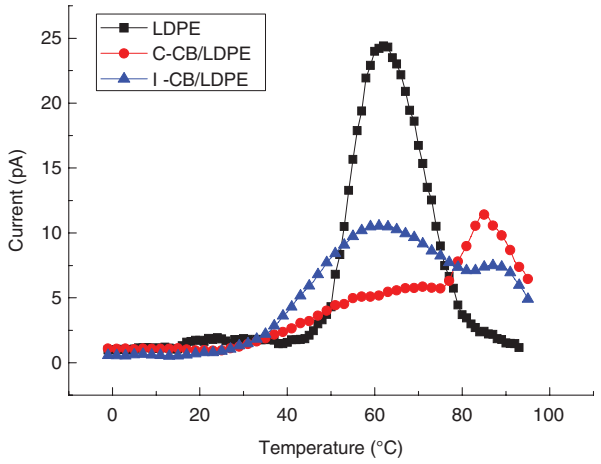

Figure 7: The TSC curves of LDPE and CB/LDPE nanocomposites.

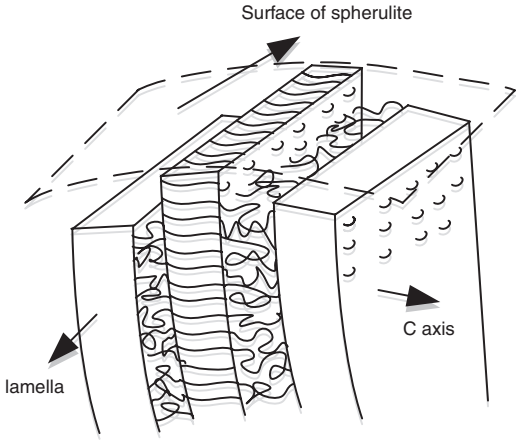

Figure 8: Diagram of spherulite structure for polyethylene.

4 Discussion

Stehling and Mandelkern (22) stated that there are three relaxation motions in polyethylene below the melting temperature. These relaxations are identified conventionally as α, β and γ relaxation in order of decreasing temperature, and each relaxation originates from a different type of molecular motion. The molecular motion can assist in the release of the space charge (23), and hence space charge release and polyethylene relaxation may have a certain correlation. The TSC current usually characterizes the thermal release process of the space charge. The TSC measurement results indicate that LDPE has a TSC current peak at about 65°C. Furthermore, the results of the DMA tests showed that the loss factor tan δ peak for LDPE also occurs at around 65°C, which characterizes the α relaxation (24). Hence, it seems probable that space charge release within LDPE is caused by α relaxation.

Polyethylene is a semi-crystalline polymer where crystalline and amorphous components are mixed. It is well known to have the spherulite structure composed of lamellae. The solid structure of polyethylene, therefore, is complicated. In order to explain the molecular motion mechanism of the α relaxation process conveniently, the structure diagram of a polyethylene spherulite is shown in Figure 8. Through analysis of the α relaxation process of semi-crystalline polyethylene and of single crystal polyethylene, Kajiyama et al. (25) demonstrated that the α relaxation in semi-crystalline polyethylene consists of two overlapping peaks, designated as the α1 and α2 relaxations. However, only one peak is observed for α relaxation in single crystal polyethylene, which is designated as the α1. Okano (26) considered that the α1 relaxation is attributable to the molecular motion within the lamellae along the c-axis (the normal direction of the lamellae) rotational and translational motions, and that the α2 relaxation is attributable to an interlamella slip process. Kakizaki and Hideshima (27) and Khanna et al. (28) considered the α relaxation to be due to the motion of the folded chain on the lamellae surfaces, and this kind of motion mechanism can also be included in the α2 relaxation. Hence, the α relaxation of polyethylene is a multiple relaxation process related to the lamellae.

Through the correlation between space charge release and α relaxation, the position information of space charge can be obtained, namely that the space charge is captured by the trap formed by molecules involved in α relaxation. In polyethylene lamellae, the molecular chains are arranged regularly and compactly, which leads to a decrease in the density of the traps. However, the surfaces of the lamellae are an active region in which there are a large number of traps, which are caused by chemical and structure defects, and thus the space charge accumulates mainly on the surfaces of the lamellae. The influence of impurities on space charge accumulation can be ignored for the LDPE samples tested in this study because the samples did not contain any additives such as cross-linking agents and/or antioxidant agents, and the preparation activities were carried out in an ultraclean environment. Therefore, the space charge accumulation in the LDPE samples was mainly due to the electrode injection. The injected electrons are captured by the traps during their migration in the LDPE matrix, which leads to space charge accumulation in the whole sample. The amount of space charge captured by the traps gradually increases with time or electrical field strength. However, both of the nanocomposites clearly could decrease the accumulation of space charge, and both exhibited excellent space charge properties compared to LDPE. The C-CB/LDPE composite had

a stronger ability to suppress space charge accumulation than did the I-CB/LDPE composite.

The CB particles, as physical cross-link points, play an important role in the LDPE matrix and the effect of the mechanism diagram is shown in Figure 9 (29). The CB particles are excluded from the amorphous region between the lamellae in the process of LDPE crystallization and produce a strong interaction with the molecular chain within the surface fold region of the lamellae, but the influence of the CB particles on the molecule in the lamellae is weak. The CB particles can inhibit the motion of the molecules around them, so both the motion activity of molecules within surface fold region of lamellae and the inter-lamellae slip motion are inhibited significantly. Therefore, the addition of CB particles can increase the rigidity, decrease the α relaxation strength and make the α relaxation peak move to a higher temperature region. The characterized results of I-CB and C-CB particles showed that the C-CB particles have more branched structures and fewer surface groups. The more branched structure can increase the number of interaction zones between the CB particles and the LDPE matrix, and the fewer surface functional groups means that there will be more unsaturated bonds at the CB particle surfaces and hence the C-CB particles are more effective as physical cross-link points, which leads the C-CB/LDPE nanocomposite having higher rigidity, lower α relaxation strength and a higher relaxation temperature, compared to the I-CB/LDPE nanocomposite.

Both LDPE and its nanocomposites have a TSC current peak at around 65°C, but for the nanocomposites, this peak is decreased in magnitude, and the variation in the TSC current peak for the nanocomposite with C-CB particles is more evident. It was observed that the value of the TSC current peak was around 65°C and the loss factor tan δ peak had similar changing trends for all three types of sample. As mentioned above, the space charge released at about 65°C was captured by traps on the surface of the lamellae. The CB particles interact with the lamella surface regions of the LDPE matrix, which causes the molecules to be arranged more compactly, and this decreases the number of structure defects and the density of the traps. Therefore, the original capture mechanism of space charge is suppressed effectively. Because the interaction between the C-CB particles and the LDPE matrix is stronger, the C-CB/LDPE nanocomposite exhibits a better space charge property than the I-CB/LDPE nanocomposite. The addition of CB particles can limit the number of structure defects participating in the α relaxation, so the ability of the nanocomposites to suppress space charge accumulation is enhanced. Additionally, a new TSC current peak occurs at approximately 85°C in both of nanocomposites, which may be attributable to the release of deeply-trapped carriers in the interface regions between the CB particles and LDPE matrix. This indicates that a new space charge capture mechanism is prompted because of the addition of CB particles. Further work is required to clarify the mechanism by which the new capture mechanism influences carrier transport behavior.

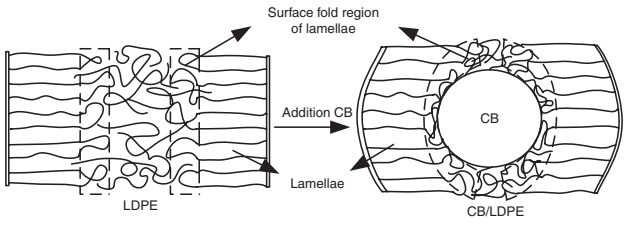

Figure 9: Effect of CB particle in the amorphous phase between lamellae crystals.

5 Conclusion

Two types of CB particles with different microstructures and surface chemical characteristics were selected as the filler phase. The mechanism of improving the space charge properties of LDPE by adding CB particles was explored during the present investigation. The conclusions can be summarized as follows:

1. The release of space charge within LDPE is due to the α relaxation, which indicates that the space charge is captured by traps formed from molecules participating in α relaxation and accumulates mainly on the surfaces of the lamellae.
2. The CB particles produce interaction with the lamella surface regions of the LDPE matrix, which causes the molecules to arrange more compactly and the number of structure defects participating in the α relaxation decreases. Therefore, the original space charge capture mechanism is suppressed effectively, due to a decrease in the density of the traps.
3. From the space charge test results it is clear that space charge accumulation can be suppressed significantly by the addition of C-CB or I-CB particles. C-CB particles with a more branched structure and fewer unsaturated bonds can produce stronger interaction with the LDPE matrix. In consequence, C-CB/LDPE type nanocomposite exhibits more excellent space charge properties compared to the I-CB/LDPE type nanocomposite.

Acknowledgments: The authors gratefully acknowledge the support of the National Natural Science Foundation of China (51337002), Natural Science Foundation for Distinguished Young Scholars of Heilongjiang Province (JC201409).

References

1. Lakshmanan P, Liang J, Jenkins N. Assessment of collection systems for HVDC connected offshore wind farms. Electr Pow Syst Res. 2015;129:75–82.
2. Yamanaka T, Maruyama S, Tanaka T. The development of DC+/-500 kV XLPE cable in consideration of the space charge accumulation. ICPADM 2003. IEEE Xplore 2003;2:689–94.
3. Montanari GC, Laurent C, Teyssedre G, Campus A. From LDPE to XLPE: investigating the change of electrical properties. Part I. space charge, conduction and lifetime. IEEE T Dielect El In. 2005;12(3):438–46.
4. Ieda M. Electrical conduction and carrier traps in polymeric materials. IEEE T Dielect El In. 1984;19(3):162–78.
5. Vanadin BV, Roy SL. Impact of concentration gradient of polarizable species on the electric field distribution in polymeric insulating material for HVDC cable. IEEE T Dielect El In. 2011;18(3):833–39.
6. Mazzanti G, Montanari GC. Electrical aging and life models: the role of space charge. IEEE T Dielect El In. 2005;12(5):876–90.
7. Fabiani D, Montanari GC, Laurent C, Teyssedre G, Morshuis PHF, Bodega R, Dissado LA. HVDC cable design and space charge accumulation. Part 3: effect of temperature gradient. IEEE Electr Insul M. 2008;24(2):5–14.
8. Fleming RJ, Ammala A, Casey PS, Lang SB. Conductivity and space charge in LDPE/$BaSrTiO_3$ nanocomposites. IEEE IEEE T Dielect El In. 2011;18(1):15–23.
9. Li ST, Zhao N, Nie YJ, Wang X, Chen G, Teyssedre G. Space charge characteristics of LDPE nanocomposite/ LDPE insulation system. IEEE T Dielect El In. 2015;22(1):92–100.
10. Tian F, Zhang J, Peng X, Hao CY. Interface trapping effects on the charge transport characteristics of LDPE/ZnO nanocomposites. IEEE T Dielect El In. 2017;24(3):1888–95.
11. Wang SJ, Zha JW, Wu YH, Ren L, Dang ZM, Wu J. Preparation, microstructure and properties of polyethylene/alumina nanocomposites for HVDC insulation. IEEE T Dielect El In. 2016;22(6):3350–6.
12. Zha JW, Wang Y, Li WK, Wang SJ, Dong ZM. Electrical properties of polypropylene/styrene-ethylene-butylene-styrene block copolymer/MgO nanocomposites. IEEE T Dielect El In. 2017;24(3):1457–64.
13. Yin Y, Li Z, Li XG, Jiang PK. Thermally stimulated currents of SiO_2/low-density polyethylene micro- and nanocomposites. IEEE T Dielect El In. 2010;5(4):385–90.
14. Tanaka T, Kozako M, Fuse N, Ohki Y. Proposal of a multi-core model for polymer nanocomposite dielectrics. IEEE T Dielect El In. 2005;12(4):669–81.
15. Lewis TJ. Interfaces are the dominant feature of dielectrics at the nanometric level. IEEE T Dielect El In. 2004;11(5):739–53.
16. Roy M, Nelson JK, Maccrone RK, Schadler LS, Reed CW, Keefe R. Polymer nanocomposite dielectrics-the role of the interface. IEEE T Dielect El In. 2005;12(4):629–43.
17. Yang JM, Liu CJ, Zheng CJ, Zhao H, Wang X, Gao MZ. Effects of interfacial charge on the DC dielectric properties of nanocomposites. J Nanomater. 2016;5:1–11.
18. Fan ZJ, Wang Y, Luo GH, Li ZF, Wei F. The synergetic effect of carbon nanotubes and carbon black in a rubber system. New Carbon Mater. 2008;46(11):149–53.
19. Shen L, Yi XS. The morphology of PE/CB conductive composites. Acta Polym Sin. 2001;1(1):130–3.
20. Toles CA, Marshall WE, Johns MM. Surface functional groups on acid-activated nutshell carbons. Carbon 1999;37(8):1207–14.
21. Wu ZS, Ye Q, Zhou YX, Zhang L, Zhang YX, Wu HZ. Conduction current and space charge characteristics of SiO_2/XLPE nanocomposites with nanoparticle surface modification. High Voltage Eng. 2014;40(10):3268–75.
22. Stehling FC, Mandelkern L. The glass temperature of linear polyethylene. Macromol. 1970;3(2):242–52.
23. Mizutani T. Behavior of charge carriers in organic insulating materials. CEIDP 2006. IEEE Xplore 2006;1–10.
24. Nitta KH, Tanaka A. Dynamic mechanical properties of metallocene catalyzed linear polyethylenes. Polymer 2001;42(3):1219–26.
25. Kajiyama T, Okada T, Sakoda A, Takayanagi M. Analysis of the α-relaxation process of bulk crystallized polyethylene based on that of single crystal mat. J Macromol Sci B. 1973;132(Part B: Physics):583–608.
26. Okano K. Theory of relaxation phenomena associated with the molecular motion in polymer crystals. J Appl Polym Sci. 2007;15(1):95–100.
27. Kakizaki M, Hideshima T. Multiple relaxation in α- and γ-loss bands of polyethylene. J Macromol Sci B. 1973;8(3):367–87.
28. Khanna YP, Turi EA, Taylor TJ, Vickroy VV, Abbott RF. Dynamic mechanical relaxations in polyethylene. Macromol. 1985;18(6):1302–9.
29. Lewis TJ. Charge transport in polyethylene nano dielectrics. IEEE T Dielect El In. 2014;21(2):497–502.